ORGANOMETALLICS
Article

Organometallics **2010,** *29,* 1157–1167 1157
DOI: 10.1021/om900984t

Bimetallic η^6,η^1 SCS- and PCP-Pincer Ruthenium Palladium Complexes: Synthesis, Structure, and Catalytic Activity

Sylvestre Bonnet,[†] Martin Lutz,[‡] Anthony L. Spek,[‡] Gerard van Koten,[†] and Robertus J. M. Klein Gebbink*[,†]

[†]*Organic Chemistry & Catalysis, Debye Institute for Nanomaterials Science, Faculty of Science, Utrecht University, Padualaan 8, 3584 CH Utrecht, The Netherlands, and* [‡]*Crystal and Structural Chemistry, Bijvoet Center for Biomolecular Research, Faculty of Science, Utrecht University, Padualaan 8, 3584 CH Utrecht, The Netherlands*

Received November 11, 2009

The synthesis of η^6,η^1 SCS- and PCP-pincer ruthenium palladium complexes $[\mathbf{3}]^+$–$[\mathbf{6}]^+$ by direct η^6-coordination of $[Ru(C_5R_5)]^+$ (R = H or Me) to the arene ring of η^1-palladated ECE-pincer ligands (E = S or P) is described. In the resulting hetero bis-organometallic complexes, the π- and σ-electrons of the ECE-pincer phenyl anion are involved in η^6- and η^1-coordination to ruthenium(II) and palladium(II), respectively. In addition to electrochemical data, which show that both metal centers are electron poor, steric effects are clearly observed by X-ray crystallography and solution NMR spectroscopy. With SCS-pincer derivatives $[\mathbf{3}]^+$ and $[\mathbf{4}]^+$, replacement of the cyclopentadienyl ligand (complex $[\mathbf{3}]^+$) by the more hindered pentamethylcyclopentadienyl ligand (complex $[\mathbf{4}]^+$) induces an inversion of the configuration of one sulfur atom in the solid state. In parallel, the dynamic inversion of configuration of the sulfur ligand observed for $[\mathbf{3}]^+$ in solution is frozen for the more hindered complex $[\mathbf{4}]^+$. Finally, preliminary catalytic studies in the cross-coupling reaction between *trans*-phenylvinylboronic acid and vinylepoxide show that, for SCS-pincer palladium complexes, η^6-coordination of $[Ru(C_5R_5)]^+$ has a positive influence on the catalytic activity of the palladium center.

Introduction

Palladium complexes are of great interest in catalysis, as they show good to excellent activity and selectivity in a wide range of carbon–carbon bond-forming reactions.[1,2] Among them, those based on the ECE-pincer ligand have been particularly well studied.[3−6] The terdentate framework of the ECE-pincer ligand stabilizes, to some extent,[7−10] the carbon-to-palladium bond. In addition, by occupying three out of the four coordination sites on the metal center, the number of catalytic intermediates is restricted, which usually improves selectivity.[11] These properties opened the door[12] to new, selective organic reactions of sensitive reagents such as allyl halides,[13] stannanes,[14] and boronic acids.[15−17]

Up to now, three different approaches have been developed to tune the catalytic activity and selectivity of ECE-pincer palladium complexes: (1) the nature of the heteroatom can be changed (E = N, S, Se, or P), which has a strong influence on the electron density, and thus the redox potential, of the palladium center;[18−20] (2) the organic substituents borne by the heteroatom can be varied, which allows for the modification of the electron-donating or electron-withdrawing properties of the pincer ligand, as well as the steric

*Corresponding author. E-mail: r.j.m.kleingebbink@uu.nl.

(1) Tsuji, J., *Palladium Reagents and Catalysts: New Perspectives for the 21st Century*; Wiley-VCH: Weinheim, Germany, 2004; p 670.
(2) Tsuji, J. *Palladium in Organic Synthesis*; Springer: Berlin, Germany, 2005; p 332.
(3) Morales-Morales, D. *The Chemistry of Pincer Compounds*; Elsevier B.V.: Amsterdam, The Netherlands, 2007; p 467.
(4) Szabó, K. *Synlett* **2006**, *6*, 811.
(5) Singleton, J. T. *Tetrahedron* **2003**, *59*, 1837.
(6) Albrecht, M.; van Koten, G. *Angew. Chem., Int. Ed.* **2001**, *40*, 3750.
(7) Yu, K. Q.; Sommer, W.; Weck, M.; Jones, C. W. *J. Catal.* **2004**, *226*, 101.
(8) Yu, K. Q.; Sommer, W.; Richardson, J. M.; Weck, M.; Jones, C. W. *Adv. Synth. Catal.* **2005**, *347*, 161.
(9) Bergbreiter, D. E.; Osburn, P. L.; Frels, J. D. *Adv. Synth. Catal.* **2005**, *347*, 172.
(10) Phan, N. T. S.; Van Der Sluys, M.; Jones, C. W. *Adv. Synth. Catal.* **2006**, *348*, 609.
(11) Solin, N.; Kjellgren, J.; Szabó, K. J. *Angew. Chem., Int. Ed.* **2003**, *42*, 3656.
(12) Selander, N.; Szabo, K. J. *Dalton Trans.* **2009**, 6267.
(13) Solin, N.; Kjellgren, J.; Szabó, K. J. *J. Am. Chem. Soc.* **2004**, *126*, 7026.
(14) Wallner, O. A.; Szabó, K. J. *Org. Lett.* **2004**, *6*, 1829.
(15) Olsson, V. J.; Sebelius, S.; Selander, N.; Szabó, K. J. *J. Am. Chem. Soc.* **2006**, *128*, 4588.
(16) Solin, N.; Wallner, O. A.; Szabó, K. J. *Org. Lett.* **2005**, *7*, 698.
(17) Kjellgren, J.; Aydin, J.; Wallner, O. A.; Saltanova, I. V.; Szabó, K. J. *Chem.—Eur. J.* **2005**, *11*, 5260.
(18) Aydin, J.; Kumar, K. S.; Eriksson, L.; Szabó, K. J. *Adv. Synth. Catal.* **2007**, *349*, 2585.
(19) Gagliardo, M.; Selander, N.; Mehendale, N. C.; van Koten, G.; Klein Gebbink, R. J. M.; Szabó, K. J. *Chem.—Eur. J.* **2007**, *14*, 4800.
(20) Gagliardo, M.; Dijkstra, H. P.; Coppo, P.; De Cola, L.; Lutz, M.; Spek, A. L.; van Klink, G. P. M.; van Koten, G. *Organometallics* **2004**, *23*, 5833.
(21) Bergbreiter, D. E.; Frels, J. D.; Rawson, J.; Li, J.; Reibenspies, J. H. *Inorg. Chim. Act.* **2006**, *359*, 1912.

Published on Web 02/10/2010

congestion around the catalytic center,[21,22] and also allows for the introduction of chirality;[23−30] and (3) substitution of the pincer arene ring at the *para*-position with respect to the carbon-to-palladium bond by electron-donating or electron-withdrawing organic groups also modifies the electron density on the palladium center.[31]

Recently,[32,33] we published a fourth approach for the functionalization of ECE-pincer palladium complexes, in which η^6-coordination of the organometallic fragment $[Ru(C_5R_5)]^+$ is realized directly to the central arene ring of the η^1-metalated pincer ligand. This one-step procedure yields stable η^6,η^1-heterobimetallic architectures sharing, in an orthogonal fashion, the σ- and π-electrons of a unique phenyl anion. Solution studies showed that in these type of complexes the $[Ru(C_5R_5)]^+$ fragment acts as a strong electron-withdrawing group on the η^1-bonded pincer metal fragment.[32,34] In a geometric sense, both faces of the pincer metal complex are dissymmetrized by η^6-coordination, which leads to planar-chiral η^6,η^1 complexes in the case of ECE′-pincer metal complexes (E ≠ E′).[33] This type of architecture is reminiscent of η^5,η^1 ferrocene- and ruthenocene-type complexes published by Brown et al.[35] and Koridze et al.,[36,37] where one of the η^5-coordinated cyclopentadienyl rings is functionalized with pincer arms and η^1-coordinated to rhodium(III) or palladium(II).

Scheme 1. Synthesis of SCS- and PCP-Pincer Ruthenium Palladium Complexes [3]$^+$−[6]$^+$

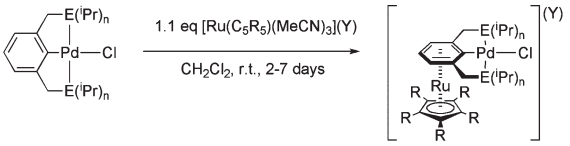

In the present study, we show that the $[Ru(C_5R_5)(MeCN)_3]^+$ arenophiles (R = H or Me)[38,39] react with SCS- and PCP-pincer palladium complexes to give the η^6,η^1-bimetallic complexes [**3**]$^+$−[**6**]$^+$ in very good isolated yields, i.e., without destabilization of the carbon-to-palladium bond. As earlier reported for NCN-pincer analogues,[32,40] electrochemical data show that the η^6-coordinated SCS- and PCP-pincer ruthenium palladium complexes [**3**]$^+$−[**6**]$^+$ are more electron poor than their monometallic precursors **1** and **2**. In addition, solid-state and solution studies clearly demonstrate that η^6-binding of the $[Ru(C_5R_5)]^+$ fragment induces steric strain between the coordination spheres of both metal centers. Finally, preliminary catalytic studies have been performed with these SCS- and PCP-pincer ruthenium palladium complexes. Our results suggest that, in the cross-coupling reaction between *trans*-phenylvinylboronic acid and vinylepoxide,[17] electronic effects cannot alone explain the trends in catalytic activity and that steric effects must also be taken into account.

Results

Synthesis. The arenophiles $[Ru(C_5R_5)(MeCN)_3]^+$ (R = H or Me)[38,39] react with SCS- and PCP-pincer palladium complexes **1**[41] and **2**[42,43] in dichloromethane at room temperature, resulting in η^6-coordination of the $[Ru(C_5R_5)]^+$ fragment to the η^1-palladated pincer arene ring. Due to the nonaromatic character of the alkyl side chains in complexes **1** and **2**, the reaction has no byproducts;[44] it slowly leads to the formation of heterobimetallic complexes [**3**]$^+$−[**6**]$^+$, which are all isolated in good yields (Scheme 1). These bimetallic complexes are remarkably stable, as they are purified by chromatography on silica gel or alumina and can be stored under ambient conditions for months.

Solid-State Structures. Single crystals suitable for X-ray diffraction were obtained for the four complexes [**3**]$^+$−[**6**]$^+$ by slow vapor diffusion of pentane or hexane into acetone or dichloromethane solutions of the complexes (see Experimental Part and Supporting Information Table S1). Selected distances and angles are given in Table 1.

(22) Gagliardo, M.; Chase, P. A.; Brouwer, S.; van Klink, G. P. M.; van Koten, G. *Organometallics* **2007**, *26*, 2219.
(23) Gosiewska, S.; Herreras, S. M.; Lutz, M.; Spek, A. L.; Havenith, R. W. A.; van Klink, G. P. M.; van Koten, G.; Klein Gebbink, R. J. M. *Organometallics* **2008**, *27*, 2549.
(24) Gosiewska, S.; Martinez, S. H.; Lutz, M.; Spek, A. L.; van Koten, G.; Klein Gebbink, R. J. M. *Eur. J. Inorg. Chem.* **2006**, 4600.
(25) Gosiewska, S.; Veld, M. F. I.; de Pater, J. J. M.; Bruijnincx, P. C. A.; Lutz, M.; Spek, A. L.; van Koten, G.; Klein Gebbink, R. J. M. *Tetrahedron: Asymmetry* **2006**, *17*, 674.
(26) Aydin, J.; Kumar, S.; Sayah, M. J.; Wallner, O. A.; Szabó, K. J. *J. Org. Chem.* **2007**, *72*, 4689.
(27) Diez-Barra, E.; Guerra, J.; Lopez-Solera, I.; Merino, S.; Rodriguez-Lopez, J.; Sanehez-Verdu, P.; Tejeda, J. *Organometallics* **2003**, *22*, 541.
(28) Stol, M.; Snelders, D. J. M.; Godbole, M. D.; Havenith, R. W. A.; Haddleton, D.; Clarkson, G.; Lutz, M.; Spek, A. L.; van Klink, G. P. M.; van Koten, G. *Organometallics* **2007**, *26*, 3985.
(29) Wallner, O. A.; Olsson, V. J.; Eriksson, L.; Szabó, K. J. *Inorg. Chim. Acta* **2006**, *359*, 1767.
(30) Albrecht, M.; Kocks, B. M.; Spek, A. L.; van Koten, G. *J. Organomet. Chem.* **2001**, *624*, 271.
(31) Dijkstra, H. P.; Slagt, M. Q.; McDonald, A.; Kruithof, C. A.; Kreiter, R.; Mills, A. M.; Lutz, M.; Spek, A. L.; Klopper, W.; van Klink, G. P. M.; van Koten, G. *Eur. J. Inorg. Chem.* **2003**, 830.
(32) Bonnet, S.; Lutz, M.; Spek, A. L.; van Koten, G.; Klein Gebbink, R. J. M. *Organometallics* **2008**, *27*, 159.
(33) Bonnet, S.; Li, J.; Siegler, M. A.; von Chrzanowski, L. S.; Spek, A. L.; van Koten, G.; Klein Gebbink, R. J. M. *Chem.—Eur. J.* **2009**, *15*, 3340.
(34) For NCN-pincer derivatives, η^6-coordination of $[Ru(C_5R_5)]^+$ to the arene ring of the pincer complex more than doubles the shift toward higher values of the irreversible Pd(II)→Pd(IV) oxidation potential, compared to a *para*-NO_2 substituent (see ref 40).
(35) Farrington, E. J.; Viviente, E. M.; Williams, B. S.; van Koten, G.; Brown, J. M. *Chem. Commun.* **2002**, 308.
(36) Koridze, A. A.; Sheloumov, A. M.; Kuklin, S. A.; Lagunova, V. Y.; Petukhova, I. I.; Dolgushin, F. M.; Ezernitskaya, M. G.; Petrovskii, P. V.; Macharashvili, A. A.; Chedia, R. V. *Russ. Chem. Bull.* **2002**, *51*, 1077.
(37) Koridze, A. A.; Kuklin, S. A.; Sheloumov, A. M.; Dolgushin, F. M.; Lagunova, V. Y.; Petukhova, I. I.; Ezernitskaya, M. G.; Peregudov, A. S.; Petrovskii, P. V.; Vorontsov, E. V.; Baya, M.; Poli, R. *Organometallics* **2004**, *23*, 4585.
(38) Fagan, P. J.; Ward, M. D.; Calabrese, J. C. *J. Am. Chem. Soc.* **1989**, *111*, 1698.
(39) Trost, B. M.; Older, C. M. *Organometallics* **2002**, *21*, 2544.
(40) Bonnet, S.; van Lenthe, J. H.; Siegler, M.; Spek, A. L.; van Koten, G.; Klein Gebbink, R. J. M. *Organometallics* **2009**, *28*, 2325.
(41) Ogo, S.; Takebe, Y.; Uehara, K.; Yamazaki, T.; Nakai, H.; Wanatabe, Y.; Fukuzumi, S. *Organometallics* **2006**, *25*, 331.
(42) Kraatz, H.-B.; Boom, M. E. v. d.; Ben-David, Y.; Milstein, D. *Isr. J. Chem.* **2001**, *41*, 163.
(43) Frech, C. M.; Shimon, L. J. W.; Milstein, D. *Angew. Chem., Int. Ed.* **2005**, *44*, 1709.
(44) When the side chain borne by the heteroatom E contained phenyl rings, nonselective η^6-coordination was observed (unpublished results). As a consequence, phenyl groups have to be avoided at that position in order to observe selective η^6-coordination to the central arene ring of the ECE-palladium pincer complex.

Table 1. Selected Distances [Å] and Angles [deg] in the Crystal Structures of $[3]^+-[6]^+$

	$[3](PF_6)$	$[4](BF_4)$	$[5](PF_6)$	$[6](BF_4)$
Ru1−Pd1	3.7029(2)	3.7383(3)	3.7969(2)	3.9323(3)
Pd1−Cl1	2.3650(4)	2.3780(7)	2.3511(4)	2.3716(6)
Pd1−C1	1.9691(16)	1.976(2)	1.9978(16)	2.011(2)
Pd1−E1	2.2832(4)	2.3033(7)	2.2819(4)	2.2798(6)
Pd1−E2	2.2949(4)	2.3037(6)	2.2890(4)	2.3217(6)
Ru1−C5R5	1.81751(13)	1.81424(19)	1.81938(14)	1.81734(18)
Ru−arene				
- to plane	1.70180(13)	1.70766(18)	1.69972(14)	1.71236(18)
- Ru1−C1	2.2337(16)	2.245(2)	2.2668(16)	2.295(2)
- Ru1−C4	2.1980(18)	2.205(2)	2.1893(17)	2.192(2)
E1−Pd1−E2	169.199(16)	170.30(2)	164.738(16)	161.17(2)
Cl1−Pd1−C1	178.12(5)	176.00(7)	173.74(5)	174.70(7)
arene−Cp angle	1.82(11)	2.72(13)	3.03(12)	6.53(13)

The molecular structures of the cations $[3]^+-[6]^+$ confirm the heterobimetallic nature of the four complexes. They unambiguously show the simultaneous η^6- and η^1-coordination of the central arene ring of the ECE-pincer ligand to, respectively, ruthenium and palladium (see Figure 1). The Ru1−Pd1 distance gradually increases from 3.7029(2) Å in $[3]^+$ to 3.9323(3) Å in $[6]^+$, while the Pd1−C1 distance concomitantly increases from 1.9691(16) Å in $[3]^+$ to 2.011(2) Å in $[6]^+$. As shown in Figure 1 there is an inversion of the configuration of one sulfur atom between $[3]^+$ and $[4]^+$, as in $[3]^+$ both ^{i}Pr substituents are in equatorial positions (racemic mixture noted $C_2(R,R)/C_2*(S,S)$: for the clarification of the notation of the stereochemistry, see Scheme 3, *vide infra*), whereas in $[4]^+$ one ^{i}Pr group is in an equatorial position and the other in an axial position (racemic $AS(S,R)/AS*(S,R)$, see Scheme 3).

In all complexes, the E−Pd−E angles are smaller than 180°, which is typical for ECE-pincer metal complexes (see Table 1). In SCS-pincer complexes $[3]^+$ and $[4]^+$, the four ligands coordinated to palladium are almost coplanar (see Table 1), whereas for PCP-pincer complexes $[5]^+$ and $[6]^+$ the η^1-bonded metal has a more distorted geometry, as P1 is clearly located out of the P2C1Pd1Cl1 plane (distance to plane: 0.5310(5) Å in $[5]^+$, 0.5922(6) Å in $[5]^+$). The conformations of the five-membered metallacycles including the Pd center are puckered for SCS-pincer complexes $[3]^+$ and $[4]^+$, with a 15.29(8)° and 10.42(11)° dihedral angle between the phenyl ring and the plane S1C1S2Pd1, respectively. As a consequence, the C_2-symmetry generally observed for SCS-pincer palladium complexes[21,45,46] is retained for the pincer fragment in $[3]^+$ and $[4]^+$. On the contrary, in PCP-pincer complexes $[5]^+$ and $[6]^+$ both phosphorus atoms are on the same side of the average arene plane, i.e., the PCP-pincer palladium fragment is in a *meso* conformation. Finally, the change in Pd−C, Pd−Cl, and Pd−S (or Pd−P) bond distances between the monometallic pincer complex **1** (or **2**) and their η^6-coordinated derivatives is small, yet significant. For example, the Pd−Cl distance is shorter in $[3]^+$ (2.3650(4) Å) and $[4]^+$ (2.3780(7) Å) than in $[PdCl(2,6\text{-}(EtSCH_2)_2C_6H_3)]$ (2.4027(8) Å).[45] In $[5]^+$ and $[6]^+$ the Pd−Cl distance is also 0.02 to 0.04 Å shorter than in $[PdCl(2,6\text{-}(^tBu_2PCH_2)_2C_6H_3)]$ (2.397(7) Å).[47] Such shortening of the Pd−Cl bond distance is consistent with a reduced *trans*-influence of the phenyl anion on the chloride ligand, hence a reduced electron density on C_{ispo}, which results from the strong electron-withdrawing properties of the η^6-coordinated ruthenium center (see also electrochemical data, *vide infra*).

In the solid state, the distance between the Ru atom and the average plane of the cyclopentadienyl ring remains in the range 1.814−1.819 Å for all complexes $[3]^+$ to $[6]^+$. Similarly, the distances between the Ru atom and the average arene plane, as well as the Ru−C_4 distances, are similar in all complexes $[3]^+$ to $[6]^+$ (see Table 1). However, the Ru1−C1 bond distance is longer than Ru1−C4 in all complexes $[3]^+$ to $[6]^+$. In addition, both the number of ^{i}Pr substituents on each heteroatom and the nature of the R group on the C_5R_5 ligand have an influence on the dihedral angle between the arene and the C_5R_5 rings. In $[3]^+$ and $[4]^+$, changing C_5H_5 into C_5Me_5 induces a small increase of the Ru1−C1 bond distance [from 2.2337(16) to 2.245(2) Å], as well as of the arene−cyclopentadienyl dihedral angle (from 1.82(11)° to 2.72(13)°). Going from $[5]^+$ to $[6]^+$ the same modification induces a large increase of the Ru1−C1 bond distance [from 2.2668(16) to 2.295(2) Å] and of the arene−cyclopentadienyl dihedral angle [from 3.03(12)° to 6.53(13)°]. The difference between the shortest (Ru−C4) and the longest (Ru−C1) bond distances in $[6]^+$ is more than 0.1 Å. As a result, the Ru−Pd distance increases from 3.7969(2) to 3.9323(3) Å. Overall, the crystal structures show the intramolecular geometric congestion between the Cp* ligand and the isopropyl groups.

Solution Structures. ^{1}H NMR spectra of bimetallic complexes $[3]^+-[6]^+$ show drastic changes compared to **1** and **2**. As documented earlier,[38] the aromatic protons of the pincer ligand are ∼0.7 ppm upfield shifted after η^6-coordination of the $[Ru(C_5R_5)]^+$ fragment, which might be due to the aromaticity of the cyclopentadienyl ligand. In addition, the persistence of the carbon-to-metal σ-bond after η^6-coordination is unequivocally shown for all complexes $[3]^+-[6]^+$ by downfield chemical shifts of the *ipso*-carbon atom in the ^{13}C NMR.[48]

The ^{1}H NMR spectrum of **2** at room temperature shows one triplet for the benzylic protons and two AB systems for the axial and equatorial ^{i}Pr methyl groups, whereas that of $[5]^+$ and $[6]^+$ shows an AB system of triplets for the benzylic protons and three ($[6]^+$) or four ($[5]^+$) well-resolved multiplets for the ^{i}Pr groups (see Figure 2). Such doubling of the signals clearly indicates that η^6-coordination to ruthenium renders the two faces of the PCP-pincer nonequivalent. The ^{1}H NMR spectra do not change upon cooling the solution to 183 K. At room temperature ^{31}P NMR gives a sharp singlet at 64.1 and 57.3 ppm for both complexes $[5]^+$ and $[6]^+$, respectively, which is consistent with an apparent symmetry of the PCP-pincer moiety in solution. All the above observations strongly support that orthogonal η^1- and η^6-coordination axes, as observed in the solid state, are retained in solution for both PCP-pincer bimetallic complexes.

In the series of SCS-pincer palladium complexes **1**, $[3]^+$, and $[4]^+$, the ^{1}H NMR patterns are more complicated due to the existence of several elements of dissymmetry (two asymmetric sulfur atoms plus the ruthenium fragment

(45) Lucena, N.; Casabó, J.; Escriche, L.; Sanchez-Castelló, G.; Teixidor, F.; Kivekäs, R.; Sillanpää, R. *Polyhedron* **1996**, *15*, 3009.

(46) Kruithof, C. A.; Dijkstra, H. P.; Lutz, M.; Spek, A. L.; Klein Gebbink, R. J. M.; van Koten, G. *Organometallics* **2008**, *27*, 4928.

(47) Kimmich, B. F. M.; Marshall, W. J.; Fagan, P. J.; Hauptman, E.; Bullock, R. M. *Inorg. Chim. Acta* **2002**, *330*, 52.

(48) The ^{13}C NMR chemical shifts δ of the *ipso* carbon are 160.4, 118.4, and 120.2 for **1**, $[3]^+$, and $[4]^+$, respectively (SCS), and 160.2, 123.3, and 128.7 for **2**, $[5]^+$, and $[6]^+$, respectively (PCP), in acetone-d_6. As observed by ^{1}H NMR for the *meta* and *para* aromatic protons, the ^{13}C NMR chemical shifts of the *ipso* carbon are upfield shifted in ruthenium-modified complexes $[3]^+-[6]^+$ compared to monometallic precursors **1** and **2**.

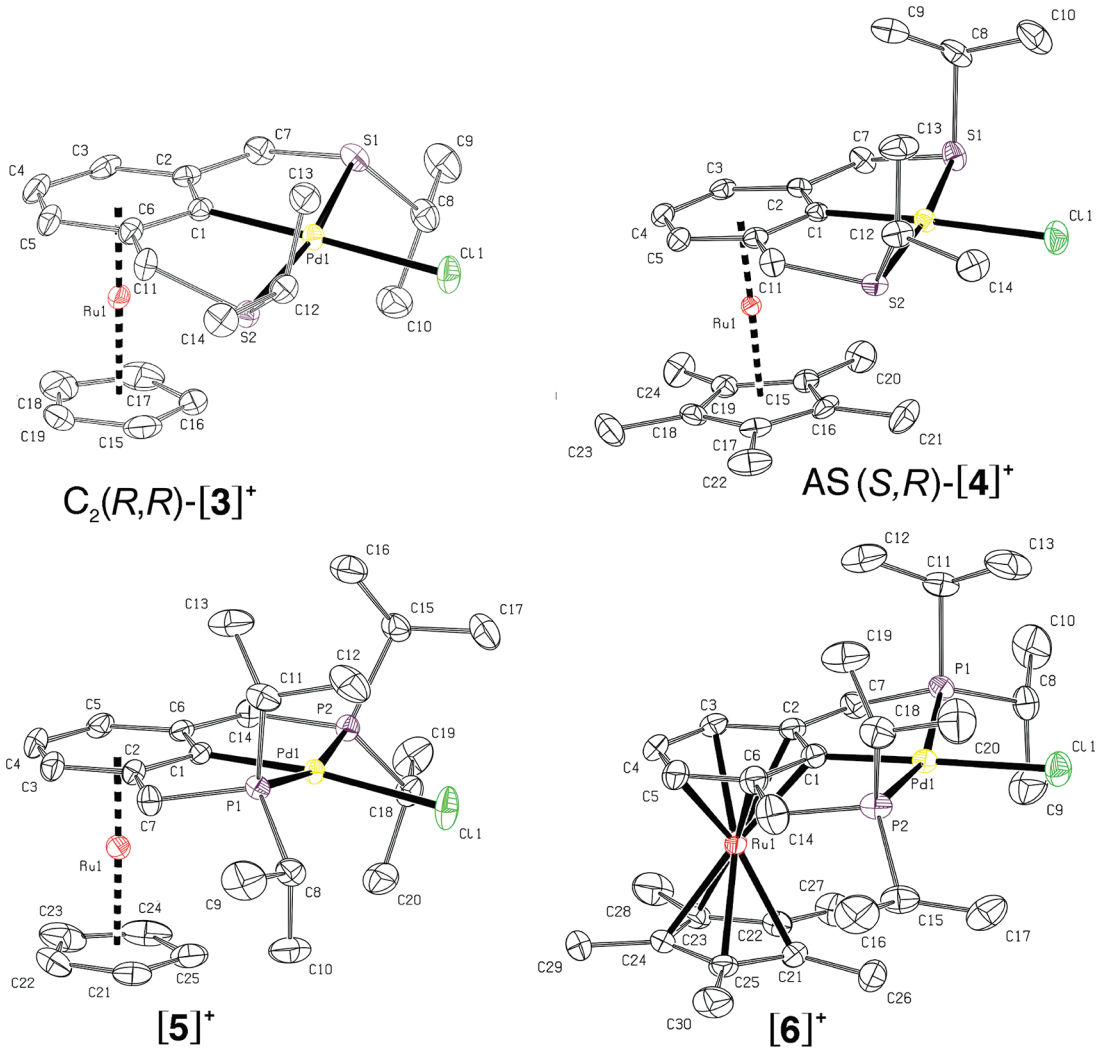

Figure 1. Displacement ellipsoid plot (drawn at 50% probability level) of complexes $[\mathbf{3}]^+$–$[\mathbf{6}]^+$. Counteranions and H atoms are omitted for clarity. The notations for the conformations of $[\mathbf{3}]^+$ and $[\mathbf{4}]^+$ are explained in Scheme 3 (*vide infra*).

inducing planar chirality) and to a more dynamic behavior in solution.[46,49,50] At room temperature in acetone, the benzylic signals are broad for **1** and $[\mathbf{3}]^+$ and sharp for $[\mathbf{4}]^+$, while the methyl signals of the ^{i}Pr groups appear as a sharp doublet for **1**, two sharp, well-resolved doublets for $[\mathbf{4}]^+$, and two doublets (one sharp, one broad) for $[\mathbf{3}]^+$. Variable-temperature NMR studies were undertaken for complexes **1**, $[\mathbf{3}]^+$, and $[\mathbf{4}]^+$ to differentiate these dynamic behaviors (see Figure 3 and Supporting Information, Figure S1). The spectrum of $[\mathbf{3}]^+$ above 313 K resembles that of $[\mathbf{4}]^+$ at room temperature, with an AB signal for the benzylic protons, two well-resolved doublets for the ^{i}Pr methyl groups, and one multiplet for the ^{i}Pr CHS signals. Such doubling of all alkyl signals is indicative of facial differentiation in $[\mathbf{3}]^+$ and $[\mathbf{4}]^+$, as already observed for PCP-pincer analogues $[\mathbf{5}]^+$ and $[\mathbf{6}]^+$. Hence orthogonal η^1- and η^6-coordination, as observed in the solid state for SCS-pincer complexes $[\mathbf{3}]^+$ and $[\mathbf{4}]^+$, is also retained in solution. Upon cooling a solution of **1** or $[\mathbf{3}]^+$, the sharp peaks observed above 313 K decoalesce at 273 K and lead, at temperatures below 233 K, to a decoalesced pattern in which several conformations have different intensities, i.e., different occupations (see Figure 3a and Supporting Information). These observations suggest a dynamic exchange between different conformations at room temperature for **1** and $[\mathbf{3}]^+$, which is frozen below 233 K in acetone. Such exchanges do not take place for $[\mathbf{4}]^+$ up to 313 K (see Figure 3b and Discussion).

In conclusion, three observations were made: (1) η^6-coordination of a $[Ru(C_5H_5)]^+$ fragment to SCS-pincer palladium complex **1** does not change the temperature dependence of the dynamic behavior of the pincer fragment in solution; (2) in contrast by η^6-coordination of a $[Ru(C_5Me_5)]^+$ fragment the inversion of configuration of the sulfur atoms is slowed down such that it does not take place at room temperature; and (3) there is no measurable dynamic behavior of PCP-pincer palladium complexes in solution between 298 and 183 K, with or without a η^6-coordinated $[Ru(C_5R_5)]^+$ fragment; that is, one preferred ring conformation is frozen.

Cyclic Voltammetry. Cyclic voltammograms of the neutral palladium (**1** and **2**) and cationic ruthenium palladium ($[\mathbf{3}]^+$–$[\mathbf{6}]^+$) complexes were recorded in acetonitrile (see Table 2). For all ECE-pincer palladium complexes (E = S or P), an irreversible oxidation wave was observed, which we attribute to Pd^{II}/Pd^{IV} oxidation as for other NCN-pincer metal compounds (E = N).[32,51–54] Generally, a clear shift of

(49) Dupont, J.; Beydoun, N.; Pfeffer, M. *Dalton Trans.* **1989**, 1715.
(50) Orrell, K. G. *Coord. Chem. Rev.* **1989**, *96*, 1.
(51) Back, S.; Gossage, R. A.; Lutz, M.; del Rio, I.; Spek, A. L.; Lang, H.; van Koten, G. *Organometallics* **2000**, *19*, 3296.

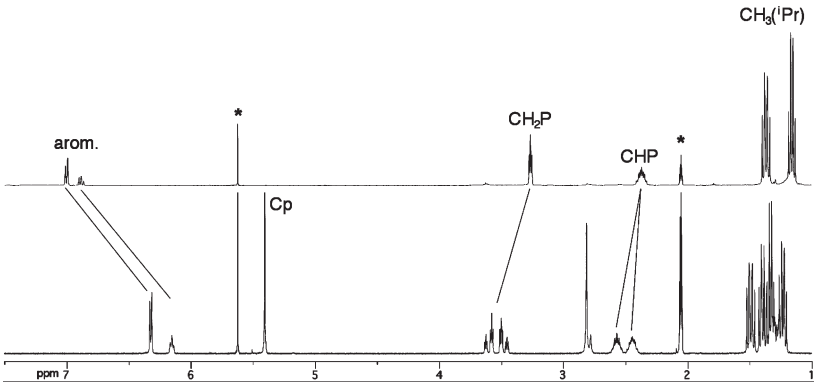

Figure 2. ^{1}H NMR spectra of **2** (top) and $[\mathbf{5}]^+$ (bottom) in acetone-d_6 at room temperature (asterisk denotes residual solvent peaks, dichloromethane and acetone).

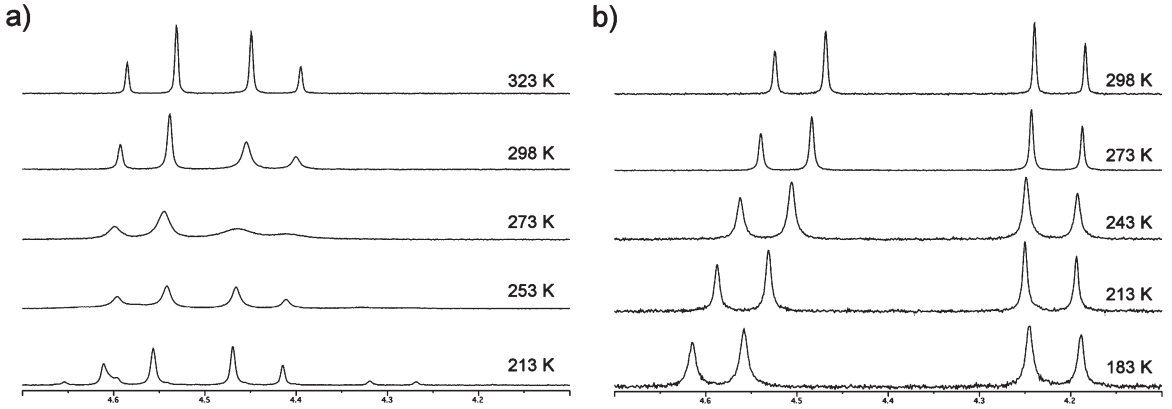

Figure 3. Variable-temperature ^{1}H NMR of complexes $[\mathbf{3}]^+$ (a) and $[\mathbf{4}]^+$ (b). Shown are the benzylic CH_2S regions: 4.1−4.7 ppm in acetone-d_6; concentrations are $\sim 4 \times 10^{-2}$ M.

this potential was observed between bimetallic and monometallic complexes. This shift is quite large for SCS-pincer complexes (ΔE_{ox} = 270 mV between $[\mathbf{3}]^+$ and **1**; ΔE_{ox} = 480 mV between $[\mathbf{4}]^+$ and **1**), but even larger for PCP-pincer complexes (ΔE_{ox} = 570 mV between $[\mathbf{6}]^+$ and **2**; ΔE_{ox} = 610 mV between $[\mathbf{5}]^+$ and **2**). Thus, in bimetallic complexes $[\mathbf{3}]^+$−$[\mathbf{6}]^+$ the electron-withdrawing effect of $[Ru(C_5R_5)]^+$ destabilizes the higher oxidation state of palladium. In addition, irreversible reductions were observed at low potentials for bimetallic complexes $[\mathbf{3}]^+$−$[\mathbf{6}]^+$, which were absent from the cyclic voltammogram of their monometallic precursors **1** and **2** (see Table 2). As irreversible reduction of ruthenium in $[Ru(\eta^6\text{-arene})(\eta^5\text{-}C_5R_5)]^+$ complexes is known to occur below −2 V in acetonitrile,[55] we interpret these reductions as Ru^{II}/Ru^{I} reductions. The reduction potentials for $[\mathbf{3}]^+$−$[\mathbf{6}]^+$ are more positive than for $[Ru(\eta^6\text{-}C_6H_6)(\eta^5\text{-}C_5R_5)]^+$ complexes, which implies that the ruthenium center is also electron poor in the bimetallic complexes. We interpret this as a competition between both metal centers for the electron density of the bridging η^6,η^1 phenylene ligand, which stabilizes the lower oxidation states both for palladium (Pd^{II}) and for ruthenium (Ru^{I}). In conclusion very strong ruthenium-to-palladium electronic interactions are observed in the heterobimetallic complexes $[\mathbf{3}]^+$−$[\mathbf{6}]^+$, which results in electron-poor metal centers (compared to monometallic analogues).

Catalysis. As a preliminary study the catalytic activity of ruthenium-modified SCS- and PCP-pincer palladium complexes $[\mathbf{3}]^+$−$[\mathbf{6}]^+$ was evaluated in the cross-coupling reaction between *trans*-phenylvinylboronic acid and vinylepoxide.[17] This reaction affords a mixture of linear and branched alcohols at room temperature in biphasic THF/water mixtures containing 2 equiv of Cs_2CO_3 (see Scheme 2, Table 3, and Figure 4). It was found that SCS-pincer palladium complexes **1**, $[\mathbf{3}]^+$, and $[\mathbf{4}]^+$ do indeed catalyze this reaction, whereas phosphine PCP-pincer palladium complexes **2**, $[\mathbf{5}]^+$, and $[\mathbf{6}]^+$ show no detectable catalytic activity even at high catalyst loading (2.5 mol %).

In order to monitor the reaction in time, the catalyst loading with SCS complexes **1**, $[\mathbf{3}]^+$, and $[\mathbf{4}]^+$ was diminished to 1 and 0.25 mol %, respectively (*note:* the use of 2.5 mol % in the original publication),[17] while the amount of water was substantially increased (+25%). Figure 4 depicts the reaction profiles as analyzed by gas chromatography, i.e., the total yields of the reaction products (linear + branched) versus time and nature of the catalyst. Table 3 gives GC yields after 10 h using 1 or 0.25 mol % of catalyst and the time (t_{50}) necessary to reach 50% conversion with 0.25 mol % of catalyst. The linear/branched ratio increases during the

(52) Gagliardo, M.; Rodriguez, G.; Dam, H. H.; Lutz, M.; Spek, A. L.; Havenith, R. W. A.; Coppo, P.; De Cola, L.; Hartl, F.; van Klink, G. P. M.; van Koten, G. *Inorg. Chem.* **2006**, *45*, 2143.
(53) Canty, A. J.; Rodemann, T.; Skelton, B. W.; White, A. H. *Organometallics* **2006**, *25*, 3996.
(54) Lagunas, M. C.; Gossage, R. A.; Spek, A. L.; van Koten, G. *Organometallics* **1998**, *17*, 731.
(55) Gusev, O. V.; Ievlev, M. A.; Peterleitner, M. G.; Peregudova, S. M.; Denisovich, L. I.; Petrovskii, P. V.; Ustynyuk, N. A. *Russ. Chem. Bull.* **1996**, *45*, 1601.

Scheme 2. Cross-Coupling Reaction between *trans*-Phenylvinylboronic Acid and Vinylepoxide (reaction 1)[a]

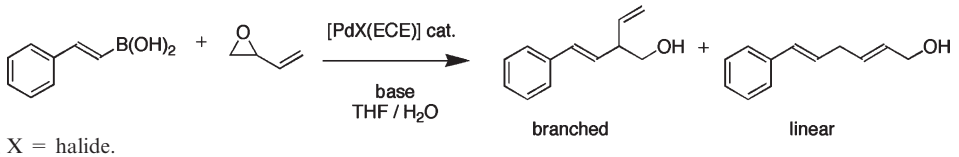

[a] E = N, S, or Se; X = halide.

Table 2. Pd^{II}/Pd^{IV} Oxidation Potentials and Ru^{II}/Ru^{I} Reduction Potentials as Measured by Cyclic Voltametry[a]

complex	$E_{ox}(Pd^{II}/Pd^{IV})$ (V)	$E_{red}(Ru^{II}/Ru^{I})$ (V)
$[Ru(C_6H_6)(Cp)]^{+}$[b]		−2.18
$[Ru(C_6H_6)(Cp^*)]^{+}$[b]		−2.48
1	+0.82	
2	+0.74	
$[\mathbf{3}]^+$	+1.09	−1.89
$[\mathbf{4}]^+$	+1.3[c]	−1.95
$[\mathbf{5}]^+$	+1.35	−2.25
$[\mathbf{6}]^+$	+1.31	−2.29

[a] Conditions: Pt electrode, scan rate 100 mV s^{-1}, 0.1 M Bu_4NPF_6 in acetonitrile, Fc/Fc^+ as internal reference. All oxidations and reductions are electrochemically irreversible. [b] See ref 55. [c] Seen as a shoulder near the solvent limit.

course of the reaction with catalyst **1**, whereas it only slightly varies with time with catalysts $[\mathbf{3}]^+$ and $[\mathbf{4}]^+$ (see Figure S4).

Discussion

Synthesis and Structure. As shown in Scheme 1, direct reaction of $[Ru(C_5R_5)(MeCN)_3]^+$ with ECE-pincer metal complexes in dichloromethane at room temperature is a very versatile reaction, as the starting metalated pincer can be any alkyl-substituted ECE-pincer metal complex having E = N, S, or P heteroatoms.[32] The η^1-palladated arene ring is electron-rich, which enhances its reactivity toward the electrophile $[Ru(C_5R_5)(MeCN)_3]^+$ under the very mild reaction conditions. Isolated yields are good to excellent, and the η^6,η^1 ruthenium palladium complexes are very stable, as they withstand column chromatography and can be stored in air for months. Such stability is remarkable, as previous work on related bis-organometallic structures have shown that rearrangements[56] or even decomposition[57] might occur. Stabilization of the σ palladium-to-carbon bond by the terdentate ECE-pincer framework[6] might also explain the peculiar stability of this family of bimetallic complexes.

Steric effects are particularly noticeable in the structures of complexes $[\mathbf{3}]^+$−$[\mathbf{6}]^+$ (see Figure 5). In the case of SCS-pincer complexes $[\mathbf{3}]^+$ and $[\mathbf{4}]^+$, each sulfur atom bears one alkyl substituent, and steric congestion is expected to be small. In the X-ray crystal structure of complex $[\mathbf{3}]^+$, the arene and cyclopentadienyl rings are almost parallel, the pincer fragment has a pseudo-C_2 symmetry, and both alkyl substituents are in equatorial position [conformation $C_2(R,R)/C_2^*(S,S)$, see Scheme 3]. For complex $[\mathbf{4}]^+$, where the cyclopentadienyl ring is substituted with five hindering methyl groups, the configuration at one sulfur atom is inversed in the solid state, which releases part of the steric strain introduced by the Cp* ligand (see Figure 5a). As a result, the bending of the arene ring with respect to the cyclopentadienyl ring remains limited in this complex (see Table 1).

PCP-pincer complexes are expected to contain more steric strain, as they bear two alkyl substituents per phosphorus atom. The *meso* conformation observed for both $[\mathbf{5}]^+$ and $[\mathbf{6}]^+$ might be taken as a sign of steric congestion (Figure 5b): the only available crystal structure of a PCP-pincer metal complex showing a *meso* conformation of the palladacycles is that of $[PdCl(2,6\text{-}(Cy_2PCH_2)_2C_6H_3)]$,[58] which bears the very bulky cyclohexyl substituents. All others PCP-pincer metal complexes, such as $[PtCl(2,6\text{-}(^iPr_2PCH_2)_2C_6H_3)]$[59] or

Table 3. Catalytic Application of SCS-Pincer Palladium Complexes 1, [3](PF6), and [4](BF4)[a]

catalyst	GC yield (%) at t = 10 h[b]	GC yield (%) at t = 10 h[c]	t_{50} (h)[c]	lin/br ratio at t = 10 h[c]
1	29	13	> 40	3.77
$[\mathbf{3}](PF_6)$	89	95	5.20	3.00
$[\mathbf{4}](BF_4)$	87	86	6.31	2.63

[a] Conditions: 1.6 mmol of boronic acid, 1.2 equiv of epoxide, 2 equiv of Cs_2CO_3, 25 °C, THF/H_2O, 7.5:1 (v/v), di(*n*-hexyl) ether (internal standard). [b] Using 1 mol % catalyst. [c] Using 0.25 mol % catalyst.

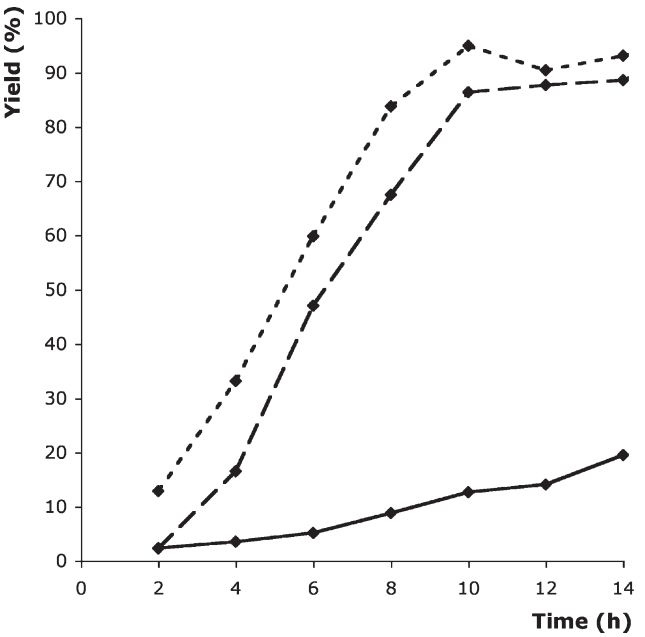

Figure 4. Total yields (linear + branched products) as a function of time in the cross-coupling reaction between *trans*-phenylvinylboronic acid and vinylepoxide, depending on the nature of the catalyst (0.25 mol %). Catalyst used: **1** (solid line), $[\mathbf{3}](PF_6)$ (dotted line), $[\mathbf{4}](BF_4)$ (dashed line).

(56) Steenwinkel, P.; James, S. L.; Gossage, R. A.; Grove, D. M.; Kooijman, H.; Smeets, W. J. J.; Spek, A. L.; van Koten, G. *Organometallics* **1998**, *17*, 4680.
(57) Winter, A. M.; Eichele, K.; Mack, H. G.; Kaska, W. C.; Mayer, H. A. *Organometallics* **2005**, *24*, 1837.
(58) Cross, R. J.; Kennedy, A. R.; Muir, K. W. *J. Organomet. Chem.* **1995**, *487*, 227.
(59) Poverenov, E.; Leitus, G.; Shimon, L. J. W.; Milstein, D. *Organometallics* **2005**, *24*, 5937.

even [PdCl(2,6-(^{t}Bu$_2$PCH$_2$)$_2$C$_6$H$_3$)],[47] show a pseudo-C_2-symmetric conformation in the solid state. The interaction between the cyclopentadienyl ring and the pincer arms in [**5**]$^+$ and [**6**]$^+$ might be the reason for such *meso* conformation in the solid state. In complex [**6**]$^+$ the arene−cyclopentadienyl dihedral angle is indeed twice as large as in complex [**5**]$^+$ [6.53(13)° vs 3.03(12)°, respectively], which is in line with the large difference observed between the Ru1−C1 and Ru1−C4 bond distances in [**6**]$^+$ [2.295(2) and 2.192(2) Å, respectively]. Such steric interactions in the solid state have earlier been reported by Koridze et al. in η^5,η^1 PCP-pincer ruthenocene palladium complexes[60] and, to a lesser extent, by ourselves for NCN-pincer ruthenium palladium analogues.[32]

The different conformations of complexes [**3**]$^+$ and [**4**]$^+$ found in the solid state are consistent with their different dynamic behavior in solution. SCS-pincer metal complexes are known to rearrange in solution according to three types of mechanisms.[46,49] First, inversion of the puckering of one metallacycle only (ring inversion, denoted (r.i.)) interconverts a C_2-symmetric geometry into a *meso* conformation, or vice versa. Second, upon inversion of the puckering of both metallacycles at the same time, wagging of the coordination plane of the metal around the carbon-to-metal bond is obtained (denoted (r.i.)^2). Third, the *R*/*S* stereochemistry of each sulfur atom is not fixed in solution; supposedly, *R* ↔ *S* epimerization occurs without decoordination of the heteroatom from the metal center (sulfur inversion, denoted (s.i.)).[61]

In case one of the faces of the arene ring of the SCS-pincer metal complex bears an η^6-coordinated [Ru(C$_5$R$_5$)]$^+$ fragment like in [**3**]$^+$ and [**4**]$^+$, the number of possible conformations is higher than for **1**. As shown in Scheme 3, starting from the C$_2$(*R*,*R*) diastereoisomer, the three new conformations AS(*R*,*S*), AS(*S*,*R*), and C$_2$(*S*,*S*) are generated by inversion of either one or two sulfur atoms. Furthermore, inversion of the puckering of both palladacycles (Δ/Λ conformations of the five-membered metallacycles) generates a further set of four conformers, which are enantiomers of one of the four starting isomers.[62] Finally, inversion of one palladacycle generates only one of the eight possible *meso* conformations (see Supporting Information): four have the two sulfur atoms on the same side as the ruthemium fragment (*syn*); four on the other side (*anti*). There are hence 16 possible conformations for complexes [**3**]$^+$ and [**4**]$^+$: eight pseudo-C_2-symmetric ones and eight *meso* ones.

At temperatures lower than 233 K in acetone, both complexes **1** and [**3**]$^+$ appear as mixtures of stereoisomers, as shown by proton NMR (see Figure 3 and Supporting Information). In the spectrum of **1** at 233 K the ^{i}Pr methyl groups give three doublets in a 1:1:2 ratio, whereas for complex [**3**]$^+$ two sets of peaks can be observed in a 1:8 ratio. Due to facial differentiation of the pincer complex in [**3**]$^+$, each isomer in Scheme 3 should give two doublets (AB pattern as a result of diastereotopic H atoms) for the benzylic protons and two doublets for the ^{i}Pr methyl peaks (as a result of diastereotopic ^{i}Pr groups; see Figure 2 and ref 32). Because coalescence is observed at 273 K in the case of **1** and [**3**]$^+$ to give a single set of signals at higher temperatures (313 K), it

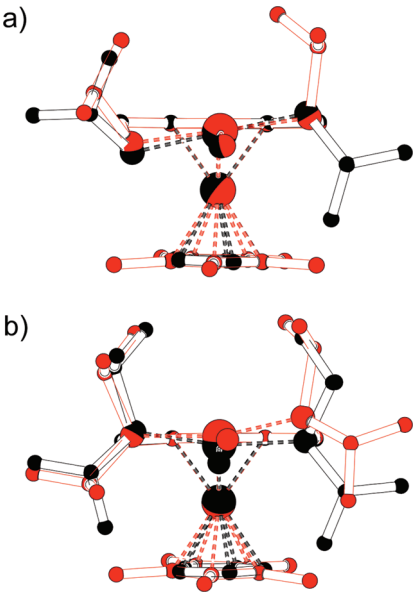

Figure 5. Quaternion fit between the molecular structures of (a) [**3**]$^+$ (black) and [**4**]$^+$ (gray) and (b) [**5**]$^+$ (black) and [**6**]$^+$ (gray), viewed from the front, i.e., along the Pd1−C1 bond. On each picture, the [Ru(η^6-arene)] fragments of the Cp and Cp* complexes have been superimposed, which visualizes the conformational differences found in the solid state upon replacing the unhindered Cp ligand by the more hindered ligand Cp*.

can be concluded that these complexes both exist as a rapidly exchanging mixture of three and two unique stereoisomers at room temperature, respectively. In contrast, [**4**]$^+$ does not show any dynamics in solution; that is, [**4**]$^+$ exists as a single stereoisomer in solution.

As the configuration of one of the sulfur atoms is inverted in [**4**]$^+$ compared to [**3**]$^+$ in the solid state, we assume that steric hindrance between the Cp* ligand and the S-alkyl substituent is also responsible for the different behaviors of complexes [**3**]$^+$ and [**4**]$^+$ in solution. Thus we interpret the NMR data as follows:

(1) For [**4**]$^+$ the unique stereoisomer detected in solution corresponds to the stereoisomer observed in the solid state, i.e., racemic AS(*S*,*R*)/AS*(*S*,*R*).

(2) The relative 1:1:2 amounts of the three stereoisomers observed for **1** at 233 K correspond to a statistical mixture of all C_2-symmetric stereoisomers, i.e., C$_2$(*R*,*R*), C$_2$(*S*,*S*), and AS(*S*,*R*) = AS(*R*,*S*), respectively.

(3) As crystals of [**3**](PF$_6$) have been grown at room temperature, we assume that the common—but not general—statement applies, that for [**3**]$^+$ the stereoisomer observed in the solid state is also the most stable one in solution; that is, the C$_2$(*R*,*R*)/C$_2$*(*S*,*S*) stereoisomer is the major species observed by ^{1}H NMR.[63] Steric interactions probably destabilize stereoisomers AS(*R*,*S*)/AS*(*R*,*S*) and C$_2$(*S*,*S*)/C$_2$*(*R*,*R*), which have one ^{i}Pr group on the same side as the [Ru(C$_5$R$_5$)]$^+$ fragment. Finally, as the different *meso* conformations would probably be of comparable stability, their simultaneous presence in solution would lead to at least five stereoisomers, which is much more than what is detected. As a result, we propose the racemic mixture AS(*S*,*R*)/AS*(*S*,*R*) to be the

(60) Kuklin, S. A.; Dolgushin, F. M.; Petrovskii, P. V.; Koridze, A. A. *Russ. Chem. Bull. Int. Ed.* **2006**, *55*, 1950.
(61) Oki, M. *Pure Appl. Chem.* **1989**, *61*, 699.
(62) For example, starting from C$_2$(*S*,*S*) ring inversion of both palladacycles generates C$_2$*(*S*,*S*), which is the enantiomer of C$_2$(*R*,*R*) (see Scheme 3).
(63) We also consider that the conformational equilibrium is not changed significantly in solution between room and low temperatures.

Scheme 3. Simplified Scheme Showing the Interconversion between the Eight Pseudo-C_2-Symmetric Conformations of Complexes $[3]^+$ and $[4]^+$[a]

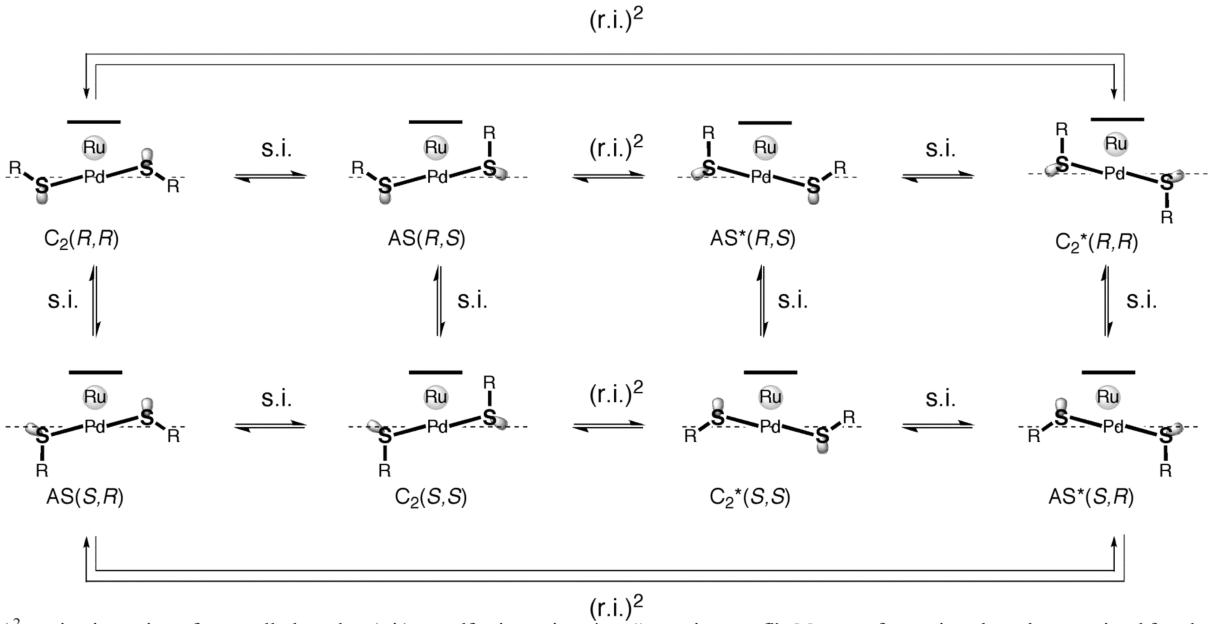

[a] (r.i.)^2 = ring inversion of two palladacycles; (s.i.) = sulfur inversion; * = "enantiomer of". *Meso* conformations have been omitted for clarity; the full scheme including the *meso* conformations can be found in the Supporting Information (Scheme S1).

minor stereoisomer detected in the ^{1}H NMR spectrum of $[3]^+$ at 233 K and below.

Catalysis. It is now clearly established that under the harsh conditions of Heck and Suzuki cross-coupling reactions (110 °C, base), SCS- and PCP-pincer palladium catalysts decompose into palladium nanoparticles, which are the real catalytically active species.[8,10,64] In the case of milder coupling reactions however, intermediate species involving simultaneously a palladium(II) center, the pincer ligand, and a vinyl or allyl ligand bound to palladium were spectroscopically detected and/or calculated by DFT methods.[11−13,18,65] In addition, the regio- or stereoselectivity observed when pincer complexes were used as catalysts was found to differ from cases where $Pd(OAc)_2$ or $Pd_2(dba)_3$ are used as catalyst precursors, which is a clear indication that the catalytically active species in such conditions is a molecular palladium complex.

Initially, the group of Szabó showed that the cross-coupling reaction between *trans*-phenylvinylboronic acid and vinylepoxide (reaction 1) was catalyzed by $[Pd_2(dba)_3]$, SeCSe-pincer, and NCN-pincer palladium complexes.[17] The reaction conditions are extremely mild (room temperature, weak base), and reactivity studies detailed in Szabó's original article showed that the mechanism with SeCSe-pincer palladium catalysts is different from that with $[Pd_2(dba)_3]$. As a consequence, decomposition of the SeCSe-pincer catalyst, thus forming palladium(0), does not occur in this reaction.

Our initial hypothesis was that the electronic effects induced by η^6-coordination of a $[Ru(C_5R_5)]^+$ cation (R = H or Me) to the arene ring of ECE-pincer palladium complexes might change the catalytic properties of the resulting complexes.[31,66,67] Such an assumption was made in relation to the mechanism proposed when E = SePh, where the rate-determining step was shown to be the nucleophilic attack of the transmetalated vinyl-palladium SeCSe-pincer intermediate [**IS**] on vinylepoxide (step 2 in Scheme 4).[17] We recently studied the catalytic activity of several NCN-pincer palladium complexes (E = NMe_2)[40] and showed that with such catalysts it is instead the transmetalation of the *trans*-phenylvinyl group from boron to palladium that is rate determining (step 1 in Scheme 4).

In comparison, the catalytic activity of SCS-pincer palladium complexes **1**, $[3]^+$, and $[4]^+$ is lower (TOF = 3−9 h^{-1}) than that of NCN-pincer analogues (TOF = 35−45 h^{-1}).[38] Complex **1** is also less active and less selective (toward the linear isomer) than [PdCl(SeCSe)] (SeCSe = $[2,6\text{-}(PhSeCH_2)_2C_6H_3]^-$).[17] The first oxidation potential of selenium being lower than that of sulfur, one might expect that selenium-based ligands behave as better σ-donating ligands than sulfur-based ones.[68] However, replacing the phenyl substituents on selenium by alkyl groups as in **1** also dramatically increases the σ-donating properties of the heteroatom.[20] As a result, the difference in terms of σ-donating properties between dialkyl SCS- and diaryl SeCSe-pincer ligands is not straightforward to predict.

Our data also clearly show that bimetallic complexes $[3]^+$ and $[4]^+$ are better catalysts than **1**. According to electrochemistry, η^6-coordination of $[Ru(C_5R_5)]^+$ to the pincer arene ring strongly increases the oxidation potential of ECE-pincer palladium complexes.[34] We expected hence a decreased electron density on palladium for $[3]^+$ and $[4]^+$, compared to **1**. Considering that an increased catalytic activity is observed for electron-poorer palladium complexes,

(64) Sommer, W.; Yu, K.; Sears, J. S.; Ji, Y.; Zheng, X.; Davis, R. J.; Sherrill, D.; Jones, C. W.; Weck, M. *Organometallics* **2005**, *24*, 4351.
(65) Kjellgren, J.; Sunden, H.; Szabo, K. J. *J. Am. Chem. Soc.* **2005**, *127*, 1787.
(66) Gottker-Schnetmann, I.; White, P.; Brookhart, M. *J. Am. Chem. Soc.* **2004**, *126*, 1804.
(67) van de Kuil, L. A.; Luitjes, H.; Grove, D. M.; Zwikker, J. W.; van der Linden, J. G. M.; Roelofsen, A. M.; Jenneskens, L. W.; Drenth, W.; van Koten, G. *Organometallics* **1994**, *13*, 468.
(68) Yao, Q.; Kinney, E. P.; Zheng, C. *Org. Lett.* **2004**, *6*, 2997.

Scheme 4. Mechanism Proposed by Szabó and Co-workers for the Cross-Coupling Reaction between *trans*-Phenylvinylboronic Acid and Vinylexpoxide[a]

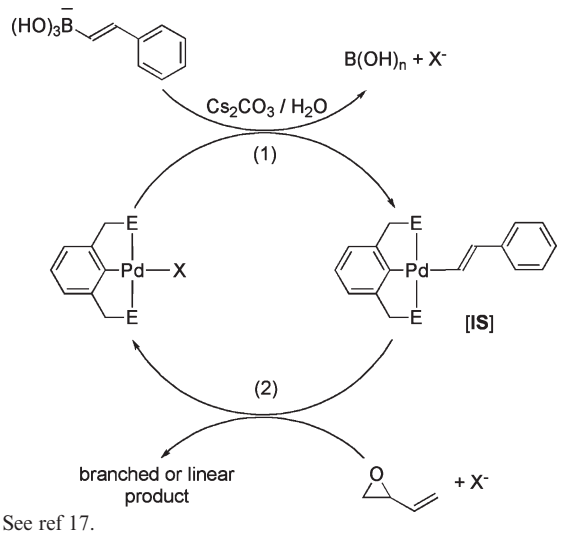

[a] See ref 17.

we assume that the nucleophilic attack of [**IS**] at vinylepoxide is not rate determining for SCS-pincer palladium catalysts. Szabó and co-workers have shown[13] that transmetalation from tin or boron derivatives to ECE-palladium pincer complexes was faster when electron density on palladium was decreased. As we observed faster reaction rates with electron-poor cationic SCS-pincer palladium complexes, we conclude that the transmetalation step is rate determining with such catalysts, as shown for NCN-pincer analogues.[40] Alternatively, with the boronic acid reagent reacting as an anionic species in basic media, the mere addition of a positive charge next to the catalytic center as in $[\mathbf{3}]^+$ and $[\mathbf{4}]^+$ might facilitate ion pair formation, hence increase the rate of the transmetalation compared to **1**.

Overall, significant differences are observed between SCS-, NCN-, phosphinite PCP-, and phosphine PCP-pincer palladium complexes. As published in Szabó's original article,[17] phosphinite PCP-pincer palladium catalysts are inactive in reaction 1, which has been attributed to a reduced electron density on palladium when coordinated by a phosphinite PCP-pincer ligand with good π-acceptor and poor σ-donor groupings. In case the palladium complex becomes too electron-deficient, nucleophilic attack of [**IS**] at the epoxide (Scheme 4) is too slow to allow reaction 1 to occur. However, in the trialkylphosphine PCP-pincer ligands the P-donor centers are not only good π-acceptors but also very good σ-donors.[20] The irreversible oxidation potential of complex **2** is only 60 mV higher than that of [PdCl(NCN)],[32] which is very electron-rich (NCN = $[2,6\text{-}(Me_2NCH_2)_2C_6H_3]^-$). Considering that the oxidation potential of **2** is intermediate between that of [PdCl(NCN)] and **1**, the absence of catalytic activity of complex **2** should not be simply attributed to electronic effects, as both [PdCl(NCN)] and **1** are catalytically active. Similarly, bimetallic complexes $[\mathbf{4}]^+$ and $[\mathbf{6}]^+$ have comparable redox potentials, but the former is catalytically active and the latter is not. Thus, the electronic character of the palladium center is not a relevant parameter to explain the absence of catalytic activity for phosphine PCP-pincer palladium complexes. We interpret the lack of catalytic activity of complexes **2**, $[\mathbf{5}]^+$, and $[\mathbf{6}]^+$ as a consequence of the higher steric congestion of the palladium center, compared to SCS- and NCN-pincer analogues. These phosphine PCP-pincer complexes bear two bulky isopropyl substituents *per* phosphorus atom, whereas SCS-pincer complexes have only one, and NCN-pincer complexes bear much smaller N-methyl substituents.[69] At the current stage of investigation it is unclear whether such increased steric congestion in phosphine PCP-pincer complexes prevents transmetalation, nucleophilic attack to the epoxide, or both in reaction 1.

Conclusion

In this work, we use the high versatility of our η^6-RuCp functionalization method for ECE-pincer metal complexes [32,33] to synthesize η^6,η^1 heterobimetallic complexes based on SCS- and PCP-pincer ligands. Complexes $[\mathbf{3}]^+$–$[\mathbf{6}]^+$ are obtained in preparative scale and very good yields[70] and are fully characterized both in the solid state and in solution. Geometrically speaking, simultaneous η^6- and η^1-coordination of two different metal centers to a single arene ring leads to relatively short metal-to-metal distances (3.7–3.9 Å). The geometrical changes observed by X-ray crystallography when the Cp ligand on ruthenium is replaced by Cp* are in line with the slowing down of the inversion of configuration of the sulfur ligands of the SCS-pincer metal complexes in solution. This clearly demonstrates the steric interactions between the pincer fragment and the bulky Cp* ligand. Modest catalytic activities were observed for SCS-pincer ruthenium palladium complexes **1**, $[\mathbf{3}]^+$, and $[\mathbf{4}]^+$ in the cross-coupling reaction 1. The higher activity of cationic complexes $[\mathbf{3}]^+$ and $[\mathbf{4}]^+$, compared to **1**, is attributed to the electron-withdrawing effects of the ruthenium center *and* to the additional positive charge borne by the bimetallic catalysts. Phosphine PCP-pincer complexes **2**, $[\mathbf{5}]^+$, and $[\mathbf{6}]^+$ are deprived of any catalytic activity in this reaction, which is attributed to the steric congestion around palladium, rather than to the electronic properties of the phosphine PCP-pincer ligand. Overall, our combined data with SCS- and PCP-pincer palladium catalysts suggest that, as recently observed for NCN-pincer palladium derivatives,[40] electronic effects are not sufficient to rationalize the catalytic activity of ECE-pincer palladium complexes and that both steric effects and the overall charge of the catalytic entity have also to be taken into account.

Experimental Part

All reactions using sensitive reagents were performed under an atmosphere of dinitrogen using Schlenk techniques. MeCN and CH_2Cl_2 were dried over CaH_2, and all solvents were freshly distilled under nitrogen prior to use. ^{1}H NMR spectra (^{1}H (300.1/400.0 MHz), ^{13}C (75.5/100.6 MHz), and $^{31}P\{^1H\}$ (121.5 MHz)) were recorded on a Varian INOVA 300 MHz spectrometer and a Varian 400 MHz spectrometer. Chemical shift values are reported in ppm (δ) relative to $(CH_3)_4Si$ (^{1}H and ^{13}C NMR) or a capillary containing 85% H_3PO_4 in D_2O ($^{31}P\{^1H\}$ NMR). MALDI-TOF mass spectra were recorded with a Bruker MicrOTOF spectrometer. Elemental analyses

(69) We recently studied the effects of steric congestion on the catalytic activity of differently hindered NCN-pincer palladium derivatives, and we made similar conclusions (see ref 40).

(70) Our functionalization method represents a good alternative for the preparation of *para*-NO_2-substituted SCS-pincer palladium complexes. Despite the large amount of work done on the preparation of functionalized SCS-pincer complexes (see for example ref 21), the *para*-NO_2-substituted one still represents an unraveled synthetic challenge.

were performed by H. Kolbe Microanalysis Laboratories, Mülheim, Germany. For column chromatography, Merck silica gel 60 (230−400 mesh) was used. Vinylepoxide, *trans*-phenylvinylboronic acid, cesium carbonate, and dihexyl ether were commercial products. SCS-pincer ligand 2,6-(^{i}PrSCH$_2$)$_2$C$_6$H$_4$,[71] PCP-pincer palladium precursor [Pd(MeCN)(PCP)](BF$_4$),[19] [Ru(C$_5$H$_5$)(MeCN)$_3$](PF$_6$),[39] and [Ru(C$_5$Me$_5$)(MeCN)$_3$](PF$_6$)[38] were prepared according to literature procedures.

Complex 1. [Pd(MeCN)$_4$](BF$_4$)$_2$ (322 mg, 1 mmol) was dissolved in dry, degassed acetonitrile (25 mL) and added under nitrogen to the ligand 2,6-(^{i}PrSCH$_2$)$_2$C$_6$H$_4$ (305 mg, 1.2 equiv). The orange mixture was heated to 50 °C under nitrogen for 16 h and turned yellow. Acetonitrile was evaporated under vacuum; distilled, degassed dichloromethane (50 mL) was added, as well as degassed brine (25 mL). The biphasic mixture was stirred vigorously for 1 h, the aqueous layer discarded, and the organic phase dried over MgSO$_4$ and evaporated. Reprecipitation from CH$_2$Cl$_2$/pentane yielded complex **1** (316 mg, 80%) that was identical to the published compound.[41] ^{1}H NMR (400 MHz; ppm in acetone-d_6): δ 6.99 (m, 3H, arom.), 4.33 (s, 4H, CH2S), 3.55 (sept, 2H, CHS(^{i}Pr), J = 6.8 Hz), 1.59 (d, 12H, CH$_3$(^{i}Pr), J = 6.8 Hz). ^{13}C NMR (100 MHz; ppm in acetone-d_6): δ_C 160.4 (*i*), 150.8 (*o*), 125.2 (*p*), 122.7 (*m*), 43.4 and 43.1 (CH$_2$S and CHS), 23.0 (CH$_3$(^{i}Pr)).

Complex 2. [Pd(MeCN)(PCP)](BF$_4$) (171 mg, 300 μmol) was dissolved in distilled, degassed dichloromethane (25 mL), and brine (20 mL) was cannulated under nitrogen. The biphasic mixture was stirred vigorously for 1 h, the aqueous phase was removed, and the organic phase was dried over MgSO$_4$. Filtration and removal of the solvent quantitatively afforded **2**, which was identical to the published compound.[42] ^{1}H NMR (400 MHz; ppm in acetone-d_6): δ 7.00 (d, 2H, m, J = 7.6), 6.88 (t, 1H, p, J = 6.9), 3.26 (t, 4H, CH$_2$P, J = 4.4), 2.37 (m, 2H, CHP), 1.36 (dd, 12H, J = 16.6, 7.2 Hz), 1.16 (dd, 12H, Me(^{i}Pr), J = 14.6, 7.1 Hz). ^{31}P NMR (162 MHz; ppm in acetone-d_6): δ 62.7. ^{13}C NMR (162 MHz; ppm in acetone-d_6): δ 160.2 (s, *i*), 151.6 (t, *ortho*, J = 10.8 Hz), 125.6 (s, *p*), 123.2 (t, *m*, J = 10.8 Hz), 33.8 (t, CHP, J = 11.6 Hz), 24.7 (t, CH$_2$P, J = 11.3 Hz), 19.1 (s, CH$_3$-(^{i}Pr)), 18.3 (CH$_3$(^{i}Pr)).

General Procedure toward Bimetallic Complexes [3]$^+$−[6]$^+$. In a typical experiment, the SCS- or PCP-pincer palladium complex **1** or **2** (250 μmol) was mixed under nitrogen with [Ru(C$_5$H$_5$)(MeCN)$_3$](PF$_6$) or [Ru(C$_5$Me$_5$)(MeCN)$_3$](BF$_4$) (275 μmol for **1**, 375 μmol for **2**) in freshly distilled dichloromethane (5.0 mL) and stirred at room temperature under nitrogen for 4 to 7 days. The dark solution was directly put on top of a 50 mL silica gel column and eluted with dichloromethane containing 1−2% methanol. Traces of starting pincer material eluted first, followed by the bimetallic complex. The product was reprecipitated from dichloromethane/pentane to yield [**3**]$^+$−[**6**]$^+$ as whitish, air-stable powders.

[3](PF$_6$): reaction time 7 days; yield 82%. ^{1}H NMR (400 MHz; ppm in acetone-d_6): δ 6.34 (d, 2H, m, J = 5.9), 6.16 (t, 1H, p, J = 5.9Hz), 5.54 (s, 5H, Cp), 4.55 (d, 2H, CH$_2$S, J = 16.2 Hz), 4.42 (d, 2H, CH$_2$S′, J = 16.6 Hz), 3.70 (sept, 2H, CHS, J = 6.8 Hz), 1.67 (d, 6H, Me, J = 6.8 Hz), 1.63 (d, 6H, Me′, J = 6.8 Hz). ^{13}C NMR (75 MHz; ppm in acetone-d_6): δ 118.4 (*i*), 113.7 (*o*), 83.5 (*p*), 83.0 (*m*), 82.1 (C^{IV} Cp), 55.0 (CH$_2$S), 44.5 and 41.3 (CHS), 23.2 and 22.8 (CH$_3$ ^{i}Pr). ^{31}P NMR (162 MHz, ppm in acetone-d_6): δ −143.16 (q, J_{F-P} = 708 Hz). MALDI-TOF m/z (calc): 421.20 (421.06, [M − PdCl + H]$^+$), 561.06 (560.92, [M]$^+$). Anal. C, H, N: 32.21/3.63/0.0 (exp) 32.30/3.71/0.0 (calc).

[4](BF$_4$): reaction time 4 days; yield 88%. ^{1}H NMR (400 MHz; acetone-d_6): δ 5.97 (d, 2H, m, J = 5.9 Hz), 5.82 (t, 1H, p, J = 5.9 Hz), 4.48 (d, 2H, CH$_2$S, J = 16.7 Hz), 4.20 (d, 2H, CH$_2$S′, J = 16.7 Hz), 3.71 (sept, 2H, CHS, J = 6.8 Hz), 2.06 (s, 15H, Cp*), 1.69 (d, 6H, Me, J = 6.8 Hz), 1.63 (d, 6H, Me′, J = 6.8 Hz). ^{13}C NMR δ(75 MHz; acetone-d_6): δ 120.2 (*i*), 113.7 (*o*), 96.8 (C^{IV} Cp*), 85.2 (*p*), 84.1 (*m*), 45.0 (CH$_2$S), 39.72 (CHS), 23.2 and 22.9 (CH$_3$ ^{i}Pr), 10.7 (Me$_5$ Cp*). ^{19}F NMR (376 MHz, acetone-d_6): δ −151.6 (s). MALDI-TOF m/z (calc): 491.25 (491.14, [M − PdCl + H]$^+$), 631.07 (631.00, [M]$^+$). Anal. C, H, N: 40.20/5.01/0.0 (exp) 40.12/5.05/0.0 (calc).

[5](PF$_6$): reaction time 7 days; yield 83%. ^{1}H NMR (400 MHz; acetone-d_6): δ 6.33 (d, 2H, *m*, J = 5.8 Hz), 6.15 (t, 1H, *p*, J = 5.8 Hz), 5.40 (s, 5H, Cp), 3.60 (dt, 2H, CH$_2$P, J = 18.6, 3.9 Hz), 3.47 (dt, 2H, CH$_2$P′, J = 18.6, 3.9 Hz), 2.57 (m, 2H, CHP), 2.44 (m, 2H, CHP′), 1.49 (m, 6H, ^{i}Pr), 1.39 (m, 6H, ^{i}Pr′), 1.33 (m, 6H, ^{i}Pr″), 1.23 (m, 6H, ^{i}Pr‴). ^{13}C NMR (100 MHz; acetone-d_6): δ 123.3 (s, *ipso*), 114.0 (t, *ortho*, J_{C-P} = 13.1 Hz), 84.2 (t, *meta*, J_{C-P} = 9.2 Hz), 84.1 (s, *para*), 81.5 (C^{IV} Cp), 55.0 (CH$_2$P, and for Me(P^{i}Pr$_2$)), 34.8 (s), 32.7 (t, J_{C-P} = 12.2 Hz), 26.7 (t, J_{C-P} = 12.0 Hz), 23.7 (t, J_{C-P} = 12.1 Hz), 23.0 (s), 19.2 (t, J_{C-P} = 2.4 Hz), 19.1 (t, J_{C-P} = 1.5 Hz), 18.58 (t, J_{C-P} = 1.9 Hz), 18.56, 17.2, 14.27. ^{19}F NMR (376 MHz, acetone-d_6): δ −67.7 (d, J_{F-P} = 708 Hz). ^{31}P NMR (162 MHz, acetone-d_6): δ 64.1 (PCP), −138.0 (q, PF$_6$, J = 708 Hz). MALDI-TOF m/z (calc): 610.25 (610.07, [M − Cl]$^+$), 645.20 (645.04, [M]$^+$). Anal. C, H, N: 37.86/5.04/0.0 (exp) 37.99/5.10/0.0 (calc).

[6](BF$_4$): reaction time 6 days; yield 85%. ^{1}H NMR (400 MHz; acetone-d_6): δ 5.94 (d, 2H, m, J = 5.8 Hz), 5.80 (t, 1H, p, J = 5.8 Hz), 3.35 (dt, 2H, CH$_2$P, J = 18.0, 4.2 Hz), 3.22 (dt, 2H, CH$_2$P′, J = 18.0, 4.2 Hz), 2.57 (m, 2H, CHP), 2.43 (m, 2H, CHP′), 1.98 (s, 15H, Cp*), 1.50 (m, 6H, ^{i}Pr), 1.39 (m, 12H, ^{i}Pr′ and ^{i}Pr″), 1.16 (m, 6H, ^{i}Pr‴). ^{13}C NMR (75 MHz; acetone-d_6): δ 128.7 (*ipso*), 111.8 (t, *ortho*, J_{C-P} = 12.6 Hz), 95.4 (C^{IV} Cp*), 85.9 (*para*), 85.3 (t, *meta*, J_{C-P} = 8.7 Hz), 55.0 (CH$_2$P), and for Me (P^{i}Pr$_2$): 31.5 (t, J_{C-P} = 11.9 Hz), 27.2 (t, J_{C-P} = 11.5 Hz), 24.2 (t, J_{C-P} = 12.0 Hz), 19.8 (t, J_{C-P} = 1.6 Hz), 19.5 (t, J_{C-P} = 2.0 Hz), 19.0 (t, J_{C-P} = 2.2 Hz), 17.6 (s), 10.5 (Me$_5$ Cp*). ^{19}F NMR (376 MHz, acetone-d_6): δ −151.4 (s). ^{31}P NMR (162 MHz, acetone-d_6): δ 57.3. MALDI-TOF m/z (calc): 679.82 (680.15, [M − Cl]$^+$), 714.85 (715.12, [M]$^+$). Anal. C, H, N: 44.98/6.25/0.0 (exp) 44.90/6.28/0.0 (calc).

X-ray Crystal Structure Determinations. X-ray reflections were measured with Mo Kα radiation (λ = 0.71073 Å) on a Nonius Kappa CCD diffractometer with rotating anode. The crystal of [**3**](PF$_6$) consisted of two crystalline fragments, but only the nonoverlapping intensities of the major fragment were used. The structures were solved with direct methods (program SHELXS-97).[72] Refinement was performed with SHELXL-97[72] against F^2 of all reflections. Non-hydrogen atoms were refined with anisotropic displacement parameters. In [**3**](PF$_6$), [**4**](BF$_4$), and [**5**](PF$_6$) all hydrogen atoms were located in difference Fourier maps. In [**6**](BF$_4$) the hydrogen atoms were introduced in calculated positions. In [**3**](PF$_6$) and [**5**](PF$_6$) the hydrogen atoms of the Ru-coordinated phenyl and cyclopentadienyl rings were refined freely with isotropic displacement parameters, and all other H atoms were refined as rigid groups. In [**4**](BF$_4$) and [**6**](BF$_4$) all hydrogen atoms were refined as rigid groups. In [**4**](BF$_4$) and [**5**](PF$_6$) the anions were refined with a disorder model using strong distance and angle restraints. Geometry calculations and checking for higher symmetry were performed with the PLATON program.[73] Further details are given in Table 1 and Table S1 (Supporting Information).

Catalytic Experiments. Eight experiments were run simultaneously using a ChemSpeed automated sampler. In each reaction vessel, Cs$_2$CO$_3$ (1.04 g, 3.2 mmol), *trans*-phenylvinylboronic acid (1.5 mL of a 1.06 M solution in tetrahydrofuran, 1.6 mmol), water (400 μL), dihexyl ether (100 μL, internal reference), and vinylexpoxide (160 μL, 1.2 equiv) were added one after another. Subsequently, 1 or 0.25 mol % of palladium catalyst was added as a solid, and the vial containing the catalyst was rinsed with 1.5 mL of tetrahydrofuran that was added to the vessel. After preparation of the eight vessels, the vessel holder was mounted on

(71) Evans, D. R.; Huang, M.; Seganish, W. M.; Chege, E. W.; Lam, Y.-F.; Fettinger, J. C.; Williams, T. L. *Inorg. Chem.* **2002**, *41*, 2633.

(72) Sheldrick, G. M. *Acta Crystallogr.* **2008**, *A64*, 112.

(73) Spek, A. L. *J. Appl. Crystallogr.* **2003**, *36*, 7.

the ChemSpeed system, and $t = 0$ was set upon starting stirring at 1000 rpm. At regular intervals stirring was stopped, the biphasic mixture was left untouched for 10 s, and 50 μL of the upper layer (THF) was taken via a syringe in each of the eight vessels and poured into 3.0 mL of dichloromethane. Stirring of the vessels was then switched on before workup of the eight samples was started. Workup consisted in adding 1.0 mL of 1 M NaOH to the dichloromethane phase and extracting it three times to remove unreacted boronic acid from the organic layer. The dichloromethane phase was analyzed by GC using dihexyl ether as internal reference.

Acknowledgment. We gratefully acknowledge the support of this research by Utrecht University and The Netherlands Research School Combination Catalysis (NRSCC). This work was supported in part (M.L., A.L.S.) by the Council for the Chemical Sciences of The Netherlands Organization for Scientific Research (CW-NWO).

Supporting Information Available: The crystal structures for complexes $[\mathbf{3}]^+-[\mathbf{6}]^+$ (in CIF format), the full variable-temperature spectra of complexes **1**, $[\mathbf{3}]^+$, and $[\mathbf{4}]^+$ in acetone-d_6 (Figures S1, S2 and S3, respectively), the full scheme containing the 16 conformations of complexes $[\mathbf{3}]^+$ and $[\mathbf{4}]^+$ (Scheme S1), the X-ray crystal structure data for complexes $[\mathbf{3}]^+-[\mathbf{6}]^+$ (Table S1), and the evolution of the linear-to-branched ratio during catalysis (Figure S4) are available free of charge via the Internet at http://pubs.acs.org.